Facile Proton-Induced Degradations of 13-Vertex Tungsta(carborane) Polyhedra[†,1]

Nicholas Carr, Donald F. Mullica, Eric L. Sappenfield, and F. Gordon A. Stone*

Department of Chemistry, Baylor University, Waco, Texas 76798-7348

Received November 12, 1992

Protonation ($HBF_4 \cdot Et_2O$) of the 13-vertex alkylidyne(carborane)tungsten salts $[NEt_4][W(\equiv CR)(CO)_2(\eta^6\text{-}7,9\text{-}R'_2\text{-}7,9\text{-}C_2B_{10}H_{10})]$ (**6**, R = C_6H_4Me-4, Me; R′ = H, Me) with 1 mol equiv of acid in the presence of donor molecules L (CO, $PhC\equiv CPh$, PPh_3), gives neutral 13- or 12-vertex tungstacarborane species, depending on the nature of L. The 13-vertex WC_2B_{10} products have the general formula $[W(CO)_2(L)_n\{\eta^6\text{-}7,9\text{-}R'_2\text{-}7,9\text{-}C_2B_{10}H_9\text{-}11\text{-}(CH_2R)\}]$ (**8a**, L = CO, R = C_6H_4Me-4, R′ = Me, *n* = 2; **8b**, L = $PhC\equiv CPh$, R = C_6H_4Me-4, R′ = Me, *n* = 1; **8c**, L = $PhC\equiv CPh$, R = Me, R′ = Me, *n* = 1) and result from migration and insertion into a B–H bond of an initially formed alkylidene {C(H)R} group. These compounds are thermally unstable, slowly decomposing in CH_2Cl_2 solution to give the 12-vertex WC_2B_9 species $[W(CO)_2(L)_n(\eta^5\text{-}7,9\text{-}R'_2\text{-}7,9\text{-}C_2B_9H_9)]$ (**9a**, L = CO, R′ = Me, *n* = 2; **9b**, L = $PhC\equiv CPh$, R′ = Me, *n* = 1), a process involving formal loss of both a BH fragment and a CHR moiety. For the particular case where L = PPh_3, transformation of the WC_2B_{10} framework is so rapid that the only species isolated by protonating the alkylidyne(carborane) salts are the compounds $[W(CO)_2(PPh_3)_2(\eta^5\text{-}7,9\text{-}R'_2\text{-}7,9\text{-}C_2B_9H_9)]$ (**9c**, R′ = Me; **9d**, R′ = H) having the 2,1,7-WC_2B_9 cage framework. In the absence of substrate molecules, protonation of the species **6** with ca. 0.5 mol equiv of $HBF_4 \cdot Et_2O$ gives the ditungsten compounds $[NEt_4][W_2\{\mu\text{-}\eta^2\text{-}C(R)CO\}(CO)_3(\eta^6\text{-}7,9\text{-}R'_2\text{-}7,9\text{-}C_2B_{10}H_{10})\{\eta^6\text{-}7,9\text{-}R'_2\text{-}7,9\text{-}C_2B_{10}H_9\text{-}11\text{-}(CH_2R)\}]$ (**10**). The structure of the complex with R = Me, R′ = Me, and $[Au(PPh_3)_2]^+$ as the cation has been established by X-ray diffraction. Crystals are triclinic, space group $P\bar{1}$ (No. 2) with *a* = 9.398(1) Å, *b* = 18.181(5) Å, *c* = 20.491(3) Å, α = 69.07(2)°, β = 88.75(1)°, γ = 85.91(1)°, and *Z* = 2. The anion consists of two 13-vertex WC_2B_{10} metallacarboranes connected by a W–W bond [2.778(1) Å] bridged by a $\mu\text{-}\eta^2$-C(Me)CO ketenyl ligand [μ-C–W 2.22(1) and 2.27(1) Å, W–CO 2.44(2) Å], and a three-center two-electron B–H⇀W linkage. The metallacarborane cage which does not form the exopolyhedral B–H⇀W bond carries a CH_2Me substituent at the boron atom that is in a β site with respect to the carbon atoms of the metal-ligating CBCBBB ring. In addition to the X-ray crystal structure determination, the IR and NMR data for the new complexes are reported and discussed.

Introduction

We have previously shown that protonation of salts of the anionic alkylidyne(carborane)tungsten complexes $[W(\equiv CR)(CO)_2(\eta^5\text{-}7,8\text{-}Me_2\text{-}7,8\text{-}C_2B_9H_9)]^-$ (**1**) (R = alkyl or aryl) with 1 mol equiv of $HBF_4 \cdot Et_2O$ in the presence of suitable Lewis base substrate molecules L, yields species of the type $[W(CO)_2(L)_2\{\eta^5\text{-}7,8\text{-}Me_2\text{-}7,8\text{-}C_2B_9H_8\text{-}10\text{-}(CH_2R)\}]$ (**2**) (R = Me, C_6H_4Me-4, or C_6H_4OMe-2; L = CO, PPh_3, $CNBu^t$, or $PhC\equiv CPh$; R = C_6H_4OMe-2, L = $PHPh_2$)[2] or $[W(CO)_3(L)\{\eta^5\text{-}7,8\text{-}Me_2\text{-}7,8\text{-}C_2B_9H_7\text{-}5,10\text{-}(CH_2C_6H_4CH_2\text{-}2)\}]$ (**3**) (L = CO or $PHPh_2$).[3] All of the compounds **2** and **3** are presumed to derive from an intermediate alkylidene species via insertion of the alkylidene ligand into the B–H bond of a neighboring vertex, thereby giving the BCH_2R group observed in all the products. Furthermore, the 12-vertex 3,1,2-WC_2B_9 carborane cage structure present in the parent alkylidyne complexes **1** is maintained in all of the products **2** and **3**.

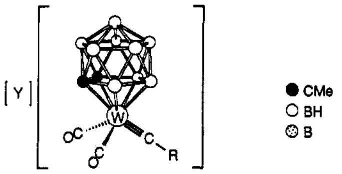

	R
1a	C_6H_4Me-4
1b	Me
1c	C_6H_4OMe-2
1d	$C_6H_4CH_2OMe$-2

Y = NEt_4, PPh_4, $AsPh_4$, NMe_3Ph, $N(PPh_3)_2$, *etc.*

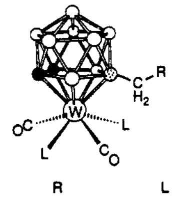

	R	L
2a	C_6H_4Me-4	CO
2b	Me	CO
2c	C_6H_4OMe-2	CO
2d	C_6H_4Me-4	PPh_3
2e	C_6H_4Me-4	PhC_2Ph

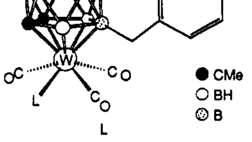

	L
3a	CO
3b	$PHPh_2$

In the absence of substrate donor molecules, treatment of **1a** with ca. 0.5 mol equiv of $HBF_4 \cdot Et_2O$ affords the

---

* To whom correspondence should be addressed.

[†] In the compounds described in this paper $[nido\text{-}7,9\text{-}C_2B_{10}H_{10}\text{-}7,9\text{-}R'_2]^{2-}$ or $[nido\text{-}7,9\text{-}C_2B_9H_9\text{-}7,9\text{-}R'_2]^{2-}$ anions form *closo*-1,6-dicarba-4- or *closo*-1,7-dicarba-2-tungstacarborane structures, respectively. However, use of this numbering scheme leads to an impossibly complex nomenclature for the dimetal compounds reported, and so we have chosen to treat the cages as *nido*-12- or -11-vertex ligands with numbering as for a docosahedron or an icosahedron, respectively, from which one vertex has been removed.

(1) Alkylidyne(carbaborane) Complexes of the Group 6 Metals. 10. Part 9: Carr, N.; Mullica, D. F.; Sappenfield, E. L.; Stone, F. G. A. *Organometallics* **1992**, *11*, 3697.

(2) (a) Brew, S. A.; Devore, D. D.; Jenkins, P. D.; Pilotti, M. U.; Stone, F. G. A. *J. Chem. Soc., Dalton Trans.* **1992**, 393. (b) Jeffery, J. C.; Li, S.; Sams, D. W. I.; Stone, F. G. A. *J. Chem. Soc., Dalton Trans.* **1992**, 877.

(3) Jeffery, J. C.; Li, S.; Stone, F. G. A. *Organometallics* **1992**, *11*, 1902.

0276-7333/93/2312-1131$04.00/0

dimetal species $[NEt_4][W_2\{\mu-\eta^2-C(C_6H_4Me-4)CO\}(CO)_2(\eta^5-7,8-Me_2-7,8-C_2B_9H_9)\{\eta^6-7,8-Me_2-7,8-C_2B_9H_8-10-(CH_2C_6H_4Me-4)\}]$ (**4**), containing a bridging η^2-ketenyl group.[1] As in the species **2**, the β boron atoms of both the cages present in **4** exhibit "noninnocent" behavior, being involved in either a B–H→W interaction or in BCH_2R group formation. Furthermore, the polyhedron bearing the $CH_2C_6H_4Me-4$ substituent displays a pronounced distortion from icosahedral geometry, due to the formal deficiency of one electron-pair. This type of hyper-closo cage geometry,[4] in which the two carbon atoms have separated such that there is no C–C connectivity, has been observed previously in (carborane)tungsten–platinum complexes.[5] The formal double bond between the two metal vertices of **4** is supported by the $C(C_6H_4Me-4)CO$ ketenyl group, as well as the B–H→W linkage. However, **4** is thermally unstable and upon heating CO is released from the ketenyl ligand to yield the alkylidyne bridged compound $[NEt_4][W_2(\mu-CC_6H_4Me-4)(CO)_2(\eta^5-7,8-Me_2-7,8-C_2B_9H_9)\{\eta^6-7,8-Me_2-7,8-C_2B_9H_8-10-(CH_2C_6H_4Me-4)\}]$ (**5**), in which the hyper-closo cage geometry present at one tungsten center in **4** is maintained.

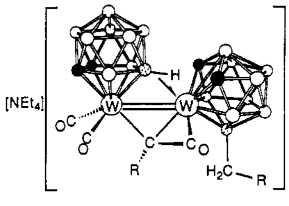

4

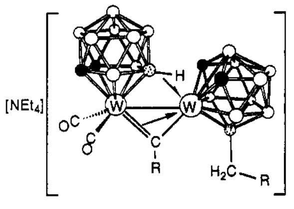

5

R = C_6H_4Me-4
● CMe
○ BH
◎ B

In view of the interesting nature of the products derived from protonation reactions of the salts **1** a natural extension of this work was to study similar experiments with the 13-vertex cage system present in the compounds $[Y][W(\equiv CR)(CO)_2(\eta^6-7,9-R'_2-7,9-C_2B_{10}H_{10})]$ (**6**) (R = C_6H_4-Me-4 or Me; R′ = H or Me). Earlier we reported[6] that the reaction between **6a** [Y = $N(PPh_3)_2$] and aqueous HX (X = Cl or I) results in degradation of the docosahedral cage system through the expulsion of one boron vertex to give the salts $[N(PPh_3)_2][WX(CO)_3(\eta^5-7,9-Me_2-7,9-C_2B_9H_9)]$ (**7**). New studies, involving protonations of the salts **6**, employing either 1 or 0.5 mol equiv of $HBF_4·Et_2O$, are described below.

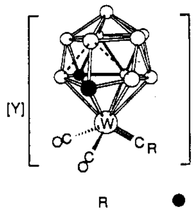

	R	●
6a	C_6H_4Me-4	CMe
6b	C_6H_4Me-4	CH
6c	Me	CMe
6d	Me	CH

Y = NEt_4 or $N(PPh_3)_2$

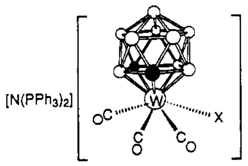

	X	● CMe
7a	Cl	
7b	I	

Results and Discussion

Carbon monoxide saturated solutions of $[NEt_4][W(\equiv CC_6H_4Me-4)(CO)_2(\eta^6-7,9-Me_2-7,9-C_2B_{10}H_{10})]$ (**6a**) upon treatment with 1 mol equiv of $HBF_4·Et_2O$ afford chromatographically inseparable mixtures of the tetracarbonyl complexes $[W(CO)_4\{\eta^6-7,9-Me_2-7,9-C_2B_{10}H_9-11-(CH_2C_6H_4Me-4)\}]$ (**8a**) and $[W(CO)_4(\eta^5-7,9-Me_2-7,9-C_2B_9H_9)]$ (**9a**). Spectroscopic measurements on freshly prepared samples of such mixtures show that initially the two species are present in ca. 4:1 ratio, respectively. However, in dichloromethane solutions, **8a** slowly mutates into **9a**, conversion being complete in ca. 2 weeks at ambient temperatures. This process involves the facile degradation of a docosahedral WC_2B_{10} cage system to an icosahedral WC_2B_9 arrangement of atoms by the extrusion of a $BCH_2C_6H_4Me-4$ fragment.

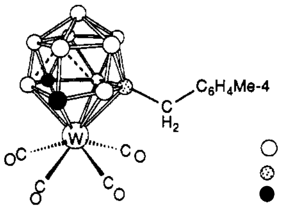

○ BH
◎ B
● CMe

8a

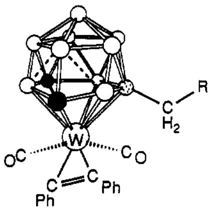

	R
8b	C_6H_4Me-4
8c	Me

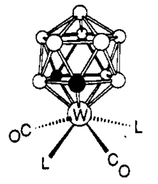

	L	●
9a	CO	CMe
9c	PPh_3	CMe
9d	PPh_3	CH

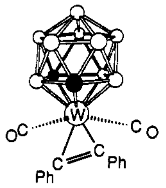

9b ● CMe

A similar pattern of behavior is observed when the salts **6a** or $[NEt_4][W(\equiv CMe)(CO)_2(\eta^6-7,9-Me_2-7,9-C_2B_{10}H_{10})]$ (**6c**) are protonated in the presence of diphenylacetylene. Thus, treatment of CH_2Cl_2 solutions of **6a** or **6c** and $PhC\equiv CPh$ with $HBF_4·Et_2O$ yields, after column chromatography, a mixture of $[W(CO)_2(\eta-PhC_2Ph)\{\eta^6-7,9-Me_2-7,9-C_2B_{10}H_9-11-(CH_2C_6H_4Me-4)\}]$ (**8b**) and $[W(CO)_2(\eta-PhC_2Ph)(\eta^5-7,9-Me_2-7,9-C_2B_9H_9)]$ (**9b**) or a mixture of $[W(CO)_2(\eta-PhC_2Ph)\{\eta^6-7,9-Me_2-7,9-C_2B_{10}H_9-11-Et\}]$ (**8c**) and **9b**, respectively. The species **8b** and **9b**, and **8c** and **9b**, are not completely separated by chromatography, and hence neither **8b** nor **8c** could be isolated free of **9b**. The compound **8b** also decomposes in solution with loss of the $BCH_2C_6H_4Me-4$ group to give **9b**, complete conversion taking ca. 1 d in refluxing CH_2Cl_2. A similar conversion of **8c** into **9b** also occurs but is accompanied by substantial decomposition to uncharacterized species.

In contrast with these results, protonation of either **6a** or **6c** in the presence of PPh_3 yields only the icosahedral complex $[W(CO)_2(PPh_3)_2(\eta^5-7,9-Me_2-7,9-C_2B_9H_9)]$ (**9c**). Similarly, a mixture of **6d**, containing cage CH vertices, and PPh_3 on treatment with $HBF_4·Et_2O$ affords only $[W(CO)_2(PPh_3)_2(\eta^5-7,9-C_2B_9H_{11})]$ (**9d**). The species **9c** is also formed by treating $[WI(CO)_3(\eta^5-7,9-Me_2-7,9-C_2B_9H_9)]$ (**7b**), the X-ray crystal structure of which has previously been determined,[6] with PPh_3 in the presence of $TlBF_4$.

---

(4) (a) Baker, R. T. *Inorg. Chem.* **1986**, *25*, 109. (b) Kennedy, J. D. *Inorg. Chem.* **1986**, *25*, 111. (c) Johnston, R. L.; Mingos, D. M. P. *Inorg. Chem.* **1986**, *25*, 3321.

(5) Attfield, M. J.; Howard, J. A. K.; Jelfs, A. N. de M.; Nunn, C. M.; Stone, F. G. A. *J. Chem. Soc., Dalton Trans.* **1987**, 2219.

(6) Brew, S. A.; Carr, N.; Jeffery, J. C.; Pilotti, M. U.; Stone, F. G. A. *J. Am. Chem. Soc.* **1992**, *114*, 2203.

Table I. Physical and Infrared Absorption Data

compd	color	yield (%)	$\nu_{max}(CO)^a/cm^{-1}$	anal. (%)[b]		
				C	H	N
6b $[N(PPh_3)_2][W(\equiv CC_6H_4Me\text{-}4)(CO)_2(\eta^6\text{-}7,9\text{-}C_2B_{10}H_{12})]$	yellow	65	1996s, 1937s	57.01 (56.20)	4.98 (4.81)	1.64 (1.37)
6c $[NEt_4][W(\equiv CMe)(CO)_2(\eta^6\text{-}7,9\text{-}Me_2\text{-}7,9\text{-}C_2B_{10}H_{10})]$	yellow	90	1987s, 1923s	34.66 (33.75)	7.52 (6.90)	2.87 (2.46)
6d $[NEt_4][W(\equiv CMe)(CO)_2(\eta^6\text{-}7,9\text{-}C_2B_{10}H_{12})]$	yellow	68	1991s, 1929s	31.63 (31.06)	6.76 (6.52)	2.87 (2.59)
8a $[W(CO)_4\{\eta^6\text{-}7,9\text{-}Me_2\text{-}7,9\text{-}C_2B_{10}H_9\text{-}11\text{-}(CH_2C_6H_4Me\text{-}4)\}]$	yellow	ca. 80[c]	2101s, 2030s, 2020s	33.27 (33.58)	4.63 (4.23)	
8b $[W(CO)_2(\eta\text{-}PhC_2Ph)\{\eta^6\text{-}7,9\text{-}Me_2\text{-}7,9\text{-}C_2B_{10}H_9\text{-}11\text{-}(CH_2C_6H_4Me\text{-}4)\}]^d$	orange	ca. 80[c]	2069s, 2021s			
8c $[W(CO)_2(\eta\text{-}PhC_2Ph)\{\eta^6\text{-}7,9\text{-}Me_2\text{-}7,9\text{-}C_2B_{10}H_9\text{-}11\text{-}Et\}]^d$	red	ca. 70[c]	2072s, 2025s			
9a $[W(CO)_4(\eta^5\text{-}7,9\text{-}Me_2\text{-}7,9\text{-}C_2B_9H_9)]$	yellow	36[e]	2094s, 2027s, 2012w, 1975s[f]	20.88 (21.06)	3.47 (3.31)	
9b $[W(CO)_2(\eta\text{-}PhC_2Ph)(\eta^5\text{-}7,9\text{-}Me_2\text{-}7,9\text{-}C_2B_9H_9)]$	purple	80	2055s, 1994s	41.24 (41.52)	4.54 (4.36)	
9c $[W(CO)_2(PPh_3)_2(\eta^5\text{-}7,9\text{-}Me_2\text{-}7,9\text{-}C_2B_9H_9)]$	yellow	93	1935s, 1845vs	53.24 (54.54)	5.03 (4.90)	
9d $[W(CO)_2(PPh_3)_2(\eta^5\text{-}7,9\text{-}C_2B_9H_{11})]$	yellow	49	1940s, 1850vs	53.30 (53.57)	4.70 (4.61)	
10a $[NEt_4][W_2\{\mu\text{-}C(C_6H_4Me\text{-}4)CO\}(CO)_3(\eta^6\text{-}7,9\text{-}Me_2\text{-}7,9\text{-}C_2B_{10}H_{10})\{\eta^6\text{-}7,9\text{-}Me_2\text{-}7,9\text{-}C_2B_{10}H_9\text{-}11\text{-}(CH_2C_6H_4Me\text{-}4)\}]$	green	21	2040s, 1991mbr, 1917mbr	37.29 (37.22)	6.16 (5.81)	1.20 (1.21)
10b $[NEt_4][W_2\{\mu\text{-}C(C_6H_4Me\text{-}4)CO\}(CO)_3(\eta^6\text{-}7,9\text{-}C_2B_{10}H_{12})\{\eta^6\text{-}7,9\text{-}C_2B_{10}H_{11}\text{-}11\text{-}(CH_2C_6H_4Me\text{-}4)\}]$	green	23	2048s, 1999m, 1963m, 1906mbr	34.62 (34.76)	5.30 (5.38)	1.26 (1.27)
10c $[NEt_4][W_2\{\mu\text{-}C(Me)CO\}(CO)_3(\eta^6\text{-}7,9\text{-}Me_2\text{-}7,9\text{-}C_2B_{10}H_{10})\{\eta^6\text{-}7,9\text{-}Me_2\text{-}7,9\text{-}C_2B_{10}H_9\text{-}11\text{-}(Et)\}]$	green	22	2035s, 1991mbr, 1913mbr	28.35 (28.55)	5.79 (5.89)	1.48 (1.39)
10d $[NEt_4][W_2\{\mu\text{-}C(Me)CO\}(CO)_3(\eta^6\text{-}7,9\text{-}C_2B_{10}H_{12})(\eta^6\text{-}7,9\text{-}C_2B_{10}H_{11}\text{-}11\text{-}Et]$	green	18	2045s, 1999m, 1966m, 1906mbr	25.41 (25.19)	5.46 (5.39)	1.43 (1.47)

[a] Measured in CH_2Cl_2 unless otherwise stated. All complexes show a weak, very broad absorption at ~2550 cm^{-1} due to cage BH stretches. [b] Calculated values in parentheses. [c] Yield estimated from spectroscopic measurements. [d] Analytically pure samples not obtained due to instability of complex (see text). [e] 75% from **2a**. [f] Measured in *n*-hexane.

This latter reaction is important since it confirms the geometry of the tungstacarborane moiety present in **9c** to be that of a 12-vertex 2,1,7-icosahedron. It would therefore appear that 13-vertex intermediate species of structural type **8** with PPh_3 ligands are too unstable for isolation. This may be due to the sterically demanding triphenylphosphine groups facilitating ejection of the BCH_2R fragments. Evidence supporting such a steric argument can be found by comparing the nature of the compounds obtained upon protonation of $[W(\equiv CC_6H_4Me\text{-}4)(CO)_2(\eta^5\text{-}7,8\text{-}Me_2\text{-}7,8\text{-}C_2B_9H_9)]$ (**1a**) or $[W(\equiv CC_6H_4OMe\text{-}2)(CO)_2(\eta^5\text{-}7,8\text{-}Me_2\text{-}7,8\text{-}C_2B_9H_9)]$ (**1c**) in the presence of PPh_3. Whereas **1c** yields $[W(CO)_3(PPh_3)\{\eta^5\text{-}7,8\text{-}Me_2\text{-}7,8\text{-}C_2B_9H_8\text{-}10\text{-}(CH_2C_6H_4OMe\text{-}2)\}]$, which contains only one phosphine molecule,[2b] the less sterically demanding C_6H_4-Me-4 carbyne substituent present in **1a** results in this species affording a mixture of the mono- and bis-phosphine complexes $[W(CO)_3(PPh_3)\{\eta^5\text{-}7,8\text{-}Me_2\text{-}7,8\text{-}C_2B_9H_8\text{-}10\text{-}(CH_2C_6H_4Me\text{-}4)\}]$ and $[W(CO)_2(PPh_3)_2\{\eta^5\text{-}7,8\text{-}Me_2\text{-}7,8\text{-}C_2B_9H_8\text{-}10\text{-}(CH_2C_6H_4Me\text{-}4)\}]$.[2a] Examination of space-filling models for these compounds, using data obtained from X-ray diffraction studies, reveal that the ligands are extremely crowded at the metal centers. However, it is noteworthy that in the absence of CO, protonation of either **6a** or **6c** with 1 mol equiv of $HBF_4{\cdot}Et_2O$ affords only **9a**, having a 12-vertex WC_2B_9 cage core structure, by scavenging of CO ligands. The implications of this latter observation for the mechanism of the docosahedral to icosahedral cage degradation are presently unclear.

Data characterizing the new compounds **8** and **9** are given in Tables I–III. As is frequently observed for compounds containing the 13-vertex MC_2B_{10} cage framework[7] the species **8** all show dynamic behavior in their NMR spectra. For **8a** low-temperature limiting spectra could not be obtained. Thus, at 190 K the signals associated with the cage CMe groups are very broad in the ^1H NMR spectrum, and only one broad signal is observed for the *C*Me nuclei in the $^{13}C\{^1H\}$ spectrum. The resonances due to the *C*Me and the BCH_2R carbon atoms are not observed, presumably due to severe broadening, and only one broad signal is seen for the four carbonyl ligands. The presence of the $BCH_2C_6H_4Me$-4 group is most clearly evident in the $^{11}B\{^1H\}$ NMR spectrum which has a signal at δ 10.9 ppm which shows no B–H coupling in a proton-coupled spectrum. In the ^{11}B NMR spectra of the alkyne complexes **8b** and **8c** the resonances due to the BCH_2R groups appear at δ 17.8 and 21.1 ppm, respectively. In accord with this, broad signals at δ 1.95 and 32.8 ppm in the ^1H and the $^{13}C\{^1H\}$ NMR spectra of **8b** are associated with the methylene group of the $CH_2C_6H_4Me$-4 substituent. The chemical shifts for the contact carbon atoms of the alkyne ligand of **8b** (δ 214.6 and 197.8 ppm) are in the range associated with four-electron donor alkyne groups,[8] as must be the case if the metal atom is to have a filled 18-electron valence shell.

In addition to the fluxionality associated with the WC_2B_{10} cage framework, variable-temperature NMR studies on compound **8c** revealed the presence of two isomers in a 1:1 ratio in solution. Thus, at 190 K two sets of signals are seen, which coalesce into the anticipated single set upon warming the solution to ca. 220 K. The similarity in chemical shift data for the two species is suggestive of geometrical isomers that are interconverting at the higher temperatures studied. The presence of two species differing solely in the disposition of the alkyne ligand with respect to the CH_2Me moiety would explain these observations, the more sterically demanding tolyl group present in **8b** favoring one particular orientation at low temperatures.

Although the CH_2R substituents in the compounds **8** are depicted as being on the boron atom that is in the site β with respect to the carbon atoms in the six-membered BCB*B*BC ring, an alternative structure in which it is either the *B*CBBBC or the BC*B*BBC boron atom that carries this substituent cannot be ruled out. However, it is evident from previous studies involving compounds of type **1** that the B–H bond β to the carbon atoms of the CCBBB pentagonal ring is invariably the most active toward insertion of alkylidene groups.[2,5] Furthermore, the X-ray

---

(7) Crennell, S. J.; Devore, D. D.; Henderson, S. J. B.; Howard, J. A. K.; Stone, F. G. A. *J. Chem. Soc., Dalton Trans.* **1989**, 1363.

(8) Templeton, J. L. *Adv. Organomet. Chem.* **1989**, *29*, 1.

Table II. Hydrogen-1 and Carbon-13 NMR Data[a]

compd	^{1}H/δ	^{13}C/δ[b]
6b	1.00 (br, 12 H, NCH$_2$*Me*), 1.75 (br, 1 H, CH), 2.16 (s, 3 H, Me-4),2.81 (br, 8 H, NC*H*$_2$Me), 5.39 (br, 1 H, CH), 7.03, 7.19 {[AB]$_2$,4 H, C$_6$H$_4$, *J*(AB) = 8}[c]	300.2 (C≡W), 211.4 (CO), 210.5 (CO), 147.2, 138.4, 128.4, 128.2 (C$_6$H$_4$), 75.7 (br, CH), 51.0 (br, N*C*H$_2$Me), 44.4 (br, CH), 21.2 (Me-4), 6.7 (NCH$_2$*Me*)[c]
6c	1.23 (br, 12 H, NCH$_2$*Me*), 1.34 (s, 3 H, CMe), 2.02, (s, 3 H, ≡CMe), 2.63 (s, 3 H, CMe), 3.11 (br, 8 H, NC*H*$_2$Me)[c]	314.1 (C≡W), 213.2 (CO), 212.3 (CO), 94.1 (br, *C*Me), 62.0 (br, *C*Me), 51.5 (br, N*C*H$_2$Me), 38.8 (≡C*Me*), 36.7 (C*Me*), 34.6 (C*Me*), 7.0 (NCH$_2$*Me*)[c]
6d	1.24 (br, 12 H, NCH$_2$*Me*), 1.62 (br, 1 H, CH), 2.06 (s, 3 H, Me), 3.12 (br, 8 H, NC*H*$_2$Me), 5.16 (br, 1 H, CH)[c]	312.2 (C≡W), 211.5 (CO), 210.7 (CO), 74.4 (br, CH), 51.5 (br, N*C*H$_2$Me), 43.4 (br, CH), 38.7 (C*Me*), 7.0 (NCH$_2$*Me*)[c]
8a	2.01 (vbr, 3 H, Me), 2.23 (s, 3 H, Me-4), 2.38 (s, 2 H, BCH$_2$), 2.86 (vbr, 3 H, Me), 6.96, 7.00 {[AB]$_2$, 4 H, C$_6$H$_4$, *J*(AB) = 7}[c]	200.8 (br, CO), 142.4, 132.7, 127.8, 127.3 (C$_6$H$_4$), 36.7 (vbr, C*Me*), 20.2 (Me–4)[c,d]
8b	1.79 (s, 3 H, Me), 1.95 (s, 2 H, BCH$_2$), 2.16 (s, 3 H, Me-4), 2.77 (s, 3 H, Me), 6.29, 6.74 {[AB]$_2$, 4 H, C$_6$H$_4$, *J*(AB) = 7}, 6.92 to 7.65 (10 H, Ph)[c]	214.6 (br, Ph*C*$_2$Ph), 206.7 (CO), 197.8 (br, Ph*C*$_2$Ph), 194.2 (CO), 141.7 to 128.6 (Ph and C$_6$H$_4$), 100.2 (br, *C*Me), 76.1 (br, *C*Me), 36.8 (C*Me*), 35.4 (C*Me*), 32.8 (br, BCH$_2$), 20.1 (Me-4)
8c	–0.39 (m, 1 H, BCH$_2$), 0.17 (br, 3 H, BCH$_2$*Me*), 0.36 (m, 5 H, B*CH*$_2$*Me*), 0.86 (m, 1 H, BCH$_2$), 2.09 (s, 3 H, Me), 2.12 (s, 3 H, Me), 2.76 (s, 3 H, CMe), 3.31 (s, 3 H, Me), 7.37 to 8.01 (20 H, Ph)[c,e]	217.5, 215.1 (vbr), 208.1, 207.3, 206.8, 201.8 (vbr), 196.9, 196.0 (4 × CO and 2 × Ph*C*$_2$Ph), 136.8 to 127.5 (Ph), 104.2 (br, *C*Me), 99.3 (br, *C*Me), 76.2 (br, *C*Me), 73.9 (br, *C*Me), 37.1 (C*Me*), 36.8 (C*Me*), 36.7 (C*Me*), 36.4 (C*Me*), 19.0 (br, BCH$_2$), 18.0 (br, BCH$_2$), 14.2 (BCH$_2$*Me*), 13.5 (BCH$_2$*Me*)[c,e]
9a	1.65 (s, Me)	208.4 [CO, *J*(WC) = 118], 73.1 (br, *C*Me), 34.9 (C*Me*)
9b	1.50 (s, 6 H, Me), 7.60 (m, 10 H, Ph)	213.5 [CO, *J*(WC) = 166], 206.0 [Ph*C*$_2$Ph, *J*(WC) = 140], 137.4, 131.4, 129.7, 128.9 (Ph), 75.0 (br, *C*Me), 32.8 (C*Me*)
9c	1.02 (s, 6 H, Me), 6.87 to 7.81 (30 H, Ph)	235.5 [t, CO, *J*(PC) = 23], 135.5 [C^4(Ph)], 130.8 [d, C^3(Ph), *J*(PC) = 20], 128.2 [d, C^2(Ph), *J*(PC) = 10], 127.9 [d, C^1(Ph), *J*(PC) = 10], 67.0 (br, *C*Me), 31.2 (C*Me*)
9d	1.71 (br, 2 H, CH), 7.35 (br, 30 H, Ph)	233.5 [t, CO, *J*(PC) = 24, *J*(WC) = 147], 135.5 (br, Ph), 133.7 (br, Ph), 131.3 (br, Ph), 128.5 (br, Ph), 51.0 (br, CH)
10a	–6.31 [q, 1 H, B–H→W, *J*(BH) = 64], 1.16 (s, 3 H, Me), 1.32 [tt, 12 H, NCH$_2$*Me*, *J*(HH) = 7, *J*(NH) = 2], 1.96 (s, 3 H, Me), 2.04, 2.40 [(AB), 2 H, BC*H*$_2$C$_6$H$_4$Me-4, *J*(AB) = 15], 2.24 (s, 3 H, Me-4), 2.25 (s, 3 H, Me-4), 2.31 (s, 3 H, Me), 2.50 (s, 3 H, Me), 3.18 [q, 8 H, NC*H*$_2$Me, *J*(HH) = 7], 6.93 to 7.10 (br, 8 H, C$_6$H$_4$)	219.6 (CO), 213.1 (CO), 202.6 (CO), 164.5 [μ-C(C$_6$H$_4$Me-4)*C*O], 145.1 to 127.8 (C$_6$H$_4$), 97.8 (br, *C*Me), 86.8 (br, *C*Me), 79.2 (br, *C*Me), 66.6 (br, *C*Me), 52.9 (br, N*C*H$_2$Me), 40.9 (br, B*C*H$_2$C$_6$H$_4$Me-4), 36.8 (C*Me*), 36.3 (C*Me*), 34.3 (C*Me*), 33.3 (C*Me*), 29.8 [μ-*C*(C$_6$H$_4$Me-4)CO], 20.9 (Me-4), 20.8 (Me-4), 7.9 (NCH$_2$*Me*)
10b	–6.34 [q, 1 H, B–H→W, *J*(BH) = 67], 1.32 [tt, 12 H, NCH$_2$*Me*, *J*(HH) = 7, J(NH) = 2], 2.25 (s, 3 H, Me-4), 2.31 (s, 3 H, Me-4), 2.32, 2.59 [(AB), 2 H, BC*H*$_2$C$_6$H$_4$Me-4, *J*(AB) = 13], 2.34 (s, 1 H, CH), 2.75 (s, 1 H, CH), 3.18 [q, 8 H, NC*H*$_2$Me, *J*(HH) = 7], 3.60 (s, 1 H, CH), 5.68 (s, 1 H, CH), 7.02 (br, 8 H, C$_6$H$_4$)	218.7 [CO, *J*(WC) = 165], 213.6 [CO, *J*(WC) = 159], 201.9 [CO, *J*(WC) 106], 160.7 [μ-C(C$_6$H$_4$Me-4)*C*O], 145.4 to 128.2 (C$_6$H$_4$), 77.0 (br, CH), 64.3 (br, CH), 61.1 (br, CH), 52.9 (br, N*C*H$_2$Me), 44.4 (br, CH), 40.7 (br, B*C*H$_2$C$_6$H$_4$Me-4), 33.8 [μ-*C*(C$_6$H$_4$Me-4)CO, *J*(WC) = 63], 21.2 (Me-4), 21.1 (Me-4), 7.9 (NCH$_2$*Me*)
10c	–6.86 [q, 1 H, B–H→W, *J*(BH) = 70], 0.85 (br, 5 H, BC*H*$_2$*Me*), 1.32 [tt, 12 H, NCH$_2$*Me*, *J*(HH) = 7, *J*(NH) = 2], 1.64 (s, 3 H, Me), 1.94 (s, 3 H, Me), 2.12 (s, 3 H, Me), 2.22 (s, 3 H, Me), 2.44 (s, 3 H, Me), 3.18 [q, 8 H, NC*H*$_2$Me, J(HH) = 7]	221.2 (CO), 216.7 (CO), 205.5 (CO), 164.1 [μ-C(Me)*C*O], 95.3 (br, *C*Me), 85.6 (br, *C*Me), 77.5 (br, *C*Me), 65.9 (br, *C*Me), 52.9 (br, N*C*H$_2$Me), 37.3 (Me), 37.1 (Me), 35.6 (Me), 32.9 (Me), 29.0 [μ-*C*(Me)CO], 25.6 (Me), 24.3 (br, B*C*H$_2$Me), 14.7 (BCH$_2$*Me*), 7.9 (NCH$_2$*Me*)
10d	–6.73 [q, 1 H, B–H→W, *J*(BH) = 72], 0.84 [t, 3 H, BCH$_2$*Me*, *J*(HH) = 7], 0.93 (m, 1 H, BC*H*$_2$Me), 1.23 (m, 1 H, BC*H*$_2$Me), 1.32 [tt, 12 H, NCH$_2$*Me*, *J*(HH) = 7, *J*(NH) = 2], 1.72 (s, 3 H, Me), 2.35 (s, 1 H, CH), 2.60 (s, 1 H, CH), 3.18 [q, 8 H, NC*H*$_2$Me, *J*(HH) = 7], 3.56 (s, 1 H, CH), 5.78 (s, 1 H, CH)	221.2 (CO), 218.6 (CO), 206.4 (CO), 159.6 [μ-C(Me)*C*O)], 75.9 (br, CH), 63.6 (br, CH), 60.0 (br, CH), 53.4 (br, N*C*H$_2$Me), 43.7 (br, CH), 24.2 (br, B*C*H$_2$Me), 21.8 [μ-*C*(Me)CO], 21.4 (Me), 14.3 (BCH$_2$*Me*), 7.9 (NCH$_2$*Me*)

[a] Measurements at ambient temperatures in CD$_2$Cl$_2$ unless otherwise stated. *J* values given in Hz. [b] Hydrogen-1 decoupled, chemical shifts are positive to high-frequency of SiMe$_4$. [c] Measured at 190 K. [d] Signal due to *C*Me nuclei not observed. [e] Two isomers present in a 1:1 ratio; as a result peaks are duplicated.

Table III. Boron-11 and Phosphorus-31 NMR Data[a]

compd	^{11}B/δ	^{31}P/δ
8a	10.9 (1 B, BCH$_2$), 4.7 (1 B, BH), 1.0 (4 B, BH), –3.6 (1 B, BH), –5.6 (2 B, BH), –7.4 (1 B, BH)	
8b	17.8 (1 B, BCH$_2$)[b]	
8c	21.1 (1 B, BCH$_2$), 6.8 (2 B, BH), 2.9 (3 B, BH), 1.3 (1 B, BH), –3.1 (2 B, BH), –5.1 (1 B, BH)	
9a	4.2 (1 B), –6.6 (1 B), –7.7 (4 B), –9.4 (2 B), –14.6 (1 B)	
9b	–1.1 (1 B), –4.8 (2 B), –7.4 (5 B), –10.4 (1 B)	
9c	–0.6 to –8.3 (br, overlapping)	15.0 [d, *J*(PP) = 29, *J*(WP) = 170], 18.3 [d, *J*(PP) = 29, *J*(WP) = 195]
9d	–3.1 (1 B), –11.8 (5 B), –17.2 (2 B), –20.1 (1 B)	29.4 [s, *J*(PW) = 190]
10a	19.4 (1 B, B–H→W, *J*(BH) = 64), 14.4 (1 B, BCH$_2$C$_6$H$_4$Me-4), 0.0 to –17.8 (18 B, BH)	
10b	21.8 (1 B, B–H→W, *J*(BH) = 67), 14.6 (1 B, BCH$_2$C$_6$H$_4$Me-4), –2.7 to –15.6 (18 B, BH)	
10c	20.2 (1 B, B–H→W, *J*(BH) = 70), 17.1 (1 B, BCH$_2$Me), 1.7 to –17.5 (18 B, BH)	
10d	22.4 (1 B, B–H→W, *J*(BH) = 72), 15.8 (1 B, BCH$_2$Me), 2.5 to –23.6 (18 B, BH)	

[a] Measurements at ambient temperatures in CD$_2$Cl$_2$. Hydrogen-1 decoupled. Chemical shifts (ppm) are positive to high frequency of BF$_3$·Et$_2$O (external) and 85% H$_3$PO$_4$ (external), respectively. [b] Signals arising from the other boron nuclei cannot be distinguished from those due to **9b**.

structural analysis described below confirms that the β B–H bond in the docosahedral salts **6** is more susceptible toward insertion of organic groups. We therefore feel confident in assigning the structure shown for the complexes **8**.

Interpretation of the NMR data (Tables II and III) for the icosahedral complexes **9a–9d** is relatively straightforward. Thus, in the ^{11}B{^{1}H} NMR spectra no especially low-field signals are present, in accord with the carborane cages in these species having terminal B–H bonds only.

For the monoalkyne complex **9b** the ligated carbon atoms of the alkyne resonate at δ 206.0 ppm, as expected for a four-electron donor ligand. It is interesting to compare the carbon-13 chemical shifts of the cage carbon atoms of the docosahedral and icosahedral species **8** and **9**, respectively. For the former structural type one of the carbon atoms is generally much more deshielded than the other (δ 100.2 and 76.1 ppm for **8b**) while for the icosahedral geometry both carbon nuclei resonate at ca. δ 70 ppm. This observation is proving to be an extremely useful aid in deducing the geometry of such metallacarborane complexes.[9]

In addition to the novel cage degradations described above, it should be noted that the alkyne complexes **8b**, **8c**, and **9b** differ from **2e**, obtained by protonating mixtures of **1a** and PhC_2Ph,[2a] in that for the latter species two alkyne molecules are coordinated to the metal, as opposed to one molecule in each of **8b**, **8c**, and **9b**. Moreover, at ambient temperatures **2e** releases CO rather than PhC_2Ph and forms the bis(alkyne)tungsten complex $[W(CO)(\eta\text{-}PhC_2Ph)_2\{\eta^5\text{-}7,8\text{-}Me_2\text{-}7,8\text{-}C_2B_9H_8\text{-}10\text{-}(CH_2C_6H_4Me\text{-}4)\}]$. This difference in reactivity is not a function of the stoichiometry of the reaction mixtures and must therefore be due to the metallacarborane cage geometry.

Protonation of the salts **6** (Y = NEt_4) with ca. 0.5 mol equiv of $HBF_4{\cdot}Et_2O$ in CH_2Cl_2 was next investigated, and in this manner the green salts $[Y][W_2\{\mu\text{-}C(R)CO\}(CO)_3(\eta^6\text{-}7,9\text{-}R'_2\text{-}7,9\text{-}C_2B_{10}H_{10})\{\eta^6\text{-}7,9\text{-}R'_2\text{-}7,9\text{-}C_2B_{10}H_9\text{-}11\text{-}(CH_2R)\}]$ (**10a**, R = C_6H_4Me-4, R′ = Me; **10b**, R = C_6H_4Me-4, R′ = H; **10c**, R = Me, R′ = Me; **10d**, R′ = Me, R = H; Y = NEt_4 for **10a**, **10b**, **10d**; Y = NEt_4 or $Au(PPh_3)_2$ for **10c**) were obtained. Data characterizing these species are listed in Tables I–III, but discussion of these results is deferred until the results of an X-ray structure determination of **10c** [Y = $Au(PPh_3)_2$] are presented. This latter salt was serendipitously formed by treating **10c** (Y = NEt_4) with $[AuCl(PPh_3)]$ in the presence of $TlBF_4$ in an attempt to prepare a neutral derivative containing an $Au(PPh_3)$ group that might afford better quality crystals for analysis by X-ray diffraction. The structure of the anion of the salt is shown in Figure 1, and selected bond distances and bond angles are collected in Table IV.

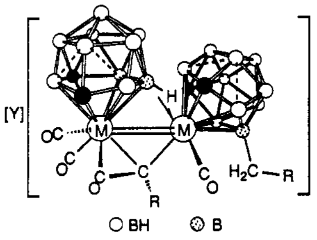

	R	●	Y
10a	C_6H_4Me-4	CMe	NEt_4
10b	C_6H_4Me-4	CH	NEt_4
10c	Me	CMe	NEt_4 or $Au(PPh_3)_2$
10d	Me	CH	NEt_4

The anion consists of two docosahedral WC_2B_{10} cage systems connected at the two metal vertices and by a three-center two-electron B–H→W linkage. The geometry of both metallacarborane cages is unchanged from that in the parent alkylidyne(carborane) anion **6c**. However, one of the cages now bears an ethyl substituent on the boron atom B(25) that is in a site β to the carbon atoms of the C(5)B(22)C(6)B(24)B(25)B(26) puckered ring. The B–H→W linkage involves the analogous boron atom B(5) in the second cage. The formal metal–metal double bond [W(1)–W(2) 2.778(1) Å] is spanned by a μ-η^2-C(Me)CO ketenyl ligand [W(1)–C(20) 2.27(1) Å, W(2)–C(20) 2.22(1) Å, W(1)–C(22) 2.44(2) Å, C(22)–O(22) 1.15(2) Å]. In addition, the metal vertex W(1) is ligated by two carbonyl groups while the other metal vertex W(2) bears only one such ligand. The mode of attachment (μ–η^2) of the ketenyl C(Me)CO group is essentially the same as found in the dimetal complex $[PtW\{\mu\text{-}C(C_6H_4Me\text{-}4)CO\}(CO)(PMe_3)(\eta^4\text{-}C_8H_{12})(\eta\text{-}C_5H_5)]$[10] and in the tetranuclear species $[RuW_3(\mu\text{-}CO)(\mu_3\text{-}\eta\text{-}CO)\{\mu\text{-}C(Ph)CO\}(\mu\text{-}CPh)(\mu_3\text{-}CPh)(CO)(PMePh_2)(\eta\text{-}C_5H_5)_3]$.[11] However, spectroscopic studies on the salts **10** indicate that in solution the ketenyl group is bound in a different manner. Thus, the solution IR spectra of the anions show no bands below 1900 cm^{-1}, but the μ–η^2 mode determined in the solid state should give rise to a C=O stretching vibration at ca. 1600–1800 cm^{-1}. Furthermore, the carbon-13 NMR chemical shifts for the ligated carbon atoms of the *C*(R)*C*O groups (ca. δ 30 and 160 ppm, respectively) are not consistent with these ligands being bound in an η^2-fashion.[12] These observations lead us to suggest that in solution there is no bond between the atoms W(1) and C(22) so that the group adopts an μ–η^1 bonding mode with the acylium resonance form, in which the ketenyl oxygen atom formally carries a positive charge and W(1) a negative charge, dominating over the alternative ketene structure.

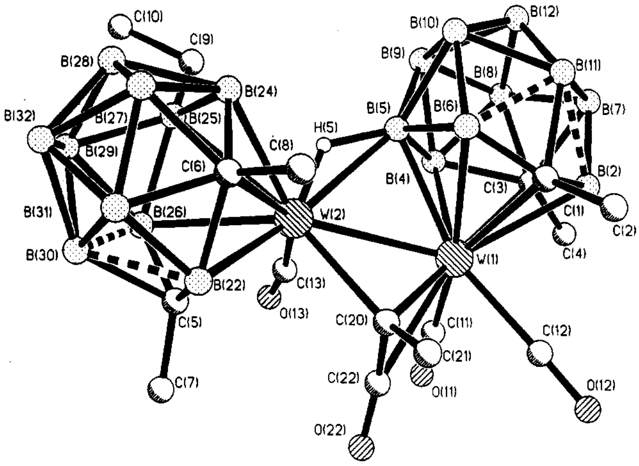

Figure 1. Structure of the anion of $[Au(PPh_3)_2][W_2\{\mu\text{-}\eta^2\text{-}C(Me)CO\}(CO)_3(\eta^6\text{-}7,9\text{-}Me_2\text{-}7,9\text{-}C_2B_{10}H_{10})\{\eta^6\text{-}7,9\text{-}Me_2\text{-}7,9\text{-}C_2B_{10}H_9\text{-}11\text{-}Et\}]$ (**10c**), showing the crystallographic labeling scheme.

The remainder of the NMR data for the salts **10** are readily interpreted. Thus, the proton-coupled ^{11}B NMR spectra all show two deshielded resonances arising from the B–H→W linkage and the BCH_2R group, the lower field one of which in each case is a doublet (J_{BH} ca. 70 Hz) and is therefore due to the boron atom involved in the three-center two-electron interaction. Correspondingly, this latter group gives rise to a broad quartet at ca. δ –6 to –7 ppm in the ^1H NMR spectrum while the BCH_2R protons are seen either as a well-resolved [AB] pattern or as complex overlapping multiplets. In addition to the signals assigned to the ketenyl ligands, the $^{13}C\{^1H\}$ NMR

---

(9) Brew, S. A.; Stone, F. G. A. *Adv. Organomet. Chem.*, in press.

(10) Jeffery, J. C.; Sambale, C.; Schmidt, M. F.; Stone, F. G. A. *Organometallics* **1982**, *1*, 1597.

(11) Farrugia, L. J.; Jeffery, J. C.; Marsden, C.; Sherwood, P.; Stone, F. G. A. *J. Chem. Soc., Dalton Trans.* **1987**, 51.

(12) Geoffroy, G. L.; Bassner, S. L. *Adv. Organomet. Chem.* **1988**, *28*, 1.

Table IV. Selected Internuclear Distances (Å) and Angles (deg) for 10c [Y = Au(PPh_3)$_2$], with Estimated Standard Deviations in Parentheses

W(1)–W(2)	2.778(1)	W(1)–C(20)	2.27(1)	W(2)–C(20)	2.22(1)	W(1)–C(22)	2.44(2)
C(20)–C(21)	1.53(2)	C(20)–C(22)	1.35(2)	C(22)–O(22)	1.15(2)	W(1)–B(5)	2.26 (1)
W(2)–B(5)	2.46(2)	W(2)–H(5)	1.43	B(5)–H(5)	1.29	W(1)–C(11)	2.03(1)
W(1)–C(12)	2.04(1)	W(2)–C(13)	1.98(1)	C(11)–O(11)	1.14(2)	C(12)–O(12)	1.13(2)
C(13)–O(13)	1.14(1)	W(1)–C(1)	2.18(1)	W(1)–C(3)	2.50(1)	W(1)–B(2)	2.45(2)
W(1)–B(4)	2.37(2)	W(1)–B(5)	2.26(1)	W(1)–B(6)	2.45(1)	W(2)–C(5)	2.23(1)
W(2)–C(6)	2.49(1)	W(2)–B(22)	2.44(1)	W(2)–B(24)	2.38(1)	W(2)–B(25)	2.51(1)
W(2)–B(26)	2.50(1)	B(25)–C(9)	1.61(2)	C(9)–C(10)	1.49(2)	B(2)–C(1)	1.60(2)
B(2)–C(3)	1.68(2)	B(2)–B(7)	1.71(3)	B(2)- - -B(11)	1.95(2)	C(3)–B(4)	1.67(2)
C(3)–B(7)	1.72(2)	C(3)–B(8)	1.68(2)	B(4)–B(5)	1.77(2)	B(4)–B(8)	1.74(2)
B(4)–B(9)	1.73(2)	B(5)–B(6)	1.85(2)	B(5)–B(9)	1.71(2)	B(5)–B(10)	1.82(2)
B(6)–C(1)	1.45(2)	B(6)–B(10)	1.81(2)	B(6)- - -B(11)	1.97(2)	C(1)–B(11)	1.83(2)
B(22)–C(5)	1.59(2)	B(22)–C(6)	1.66(2)	B(22)- - -B(30)	2.02(2)	B(22)–B(31)	1.74(2)
C(6)–B(24)	1.71(2)	C(6)–B(27)	1.71(2)	C(6)–B(31)	1.68(2)	B(24)–B(25)	1.84(2)
B(24)–B(27)	1.81(2)	B(24)–B(28)	1.78(2)	B(25)–B(26)	1.81(2)	B(25)–B(28)	1.75(2)
B(25)–B(29)	1.76(2)	B(26)–C(5)	1.62(2)	B(26)–B(29)	1.76(2)	B(26)- - -B(30)	1.95(2)
C(5)–B(30)	1.76(2)						

W(1)–W(2)–C(20)	52.5(3)	W(2)–W(1)–C(20)	51.1(3)	W(1)–C(20)–W(2)	76.5(4)
W(1)–C(20)–C(22)	80.3(7)	W(2)–C(20)–C(22)	102.7(7)	W(1)–C(20)–C(21)	126.9(8)
W(2)–C(20)–C(21)	134.4(7)	W(1)–C(22)–O(22)	134.4(8)	W(1)–C(11)–O(11)	176(1)
W(1)–C(12)–O(12)	179(1)	W(2)–C(13)–O(13)	171(1)	C(20)–C(22)–O(22)	159(1)
C(21)–C(20)–C(22)	118(1)	W(1)–B(5)–W(2)	72.0(4)	B(25)–C(9)–C(10)	117(1)

spectra each show the expected three signals due to the carbonyl groups and either eight (**10a** and **10c**) or four (**10b** and **10d**) resonances for the cage *C*Me or *C*H groups, respectively.

The mechanism for formation of these ditungsta(carborane)ketenyl complexes is subject to speculation. However, we have recently postulated[1] that the related compound **4** may be produced via an intermediate species containing a bridging alkylidene group and a terminal ketenyl group. This intermediate could result from attack of the alkylidene complex, initially formed by protonation, on unreacted alkylidyne(carborane) reagent present in the solutions. In a similar pathway, formation of an analogous intermediate from protonation of the docosahedral salts **6** followed by insertion of the C(H)R group into a B–H bond would then allow the ketenyl ligand to bridge the W–W vector giving a dinuclear species in which one metal center is electronically unsaturated, having only 16-valence electrons (**A** in Scheme I). Formation of a B–H⇀W bridge would then permit both metal centers to achieve 18-valence-electron configurations (intermediate **B**). However, formation of this linkage appears to cause the ketenyl ligand to transfer across to the other metal center to give the μ-η^2 bonding mode observed in the solid state for **6c**. The driving force for this latter transformation is presumed to be sterically based.

The difference in the nature of the products (**4** vs **10**) obtained by treament of the icosahedral species **1a**, **1b** and the docosahedral species **6** with ca. 0.5 mol equiv of $HBF_4 \cdot Et_2O$ stems from the ability of the former cage system to relieve electron deficiency by undergoing a closo to hyper-closo cage distortion. Such a transformation is not a possibility for the cage system present in anions of the salts **6**, and so these species must find an alternative means of alleviating electron shortage along the pathway to the observed products; hence the presence of three CO carbonyl ligands in the compounds **10**, as opposed to the two found in **4**.

It is noteworthy that for the species having CMe cage vertices, **6a** and **6c**, protonation with ca. 0.5 mol equiv of $HBF_4 \cdot Et_2O$ yields significant quantities of a second anionic complex. However, the nature of these species has so far proved elusive.

Scheme I. Possible Mechanism for the Formation of the Anionic Species 10

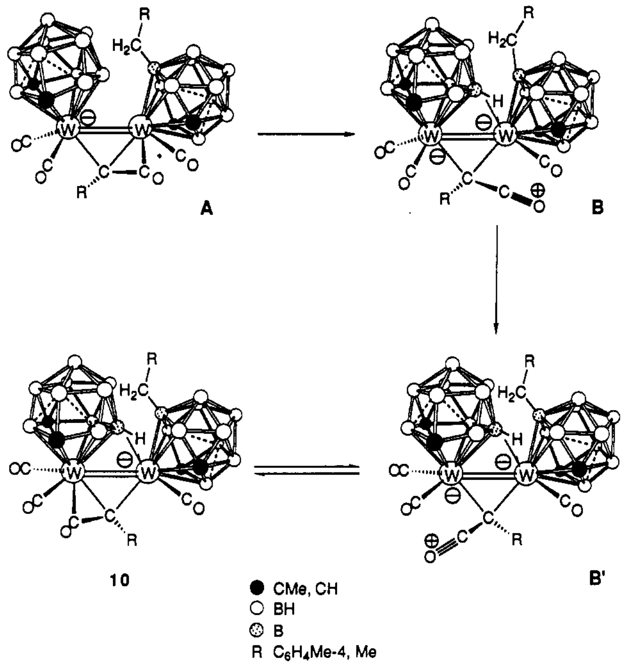

Conclusions

It is clear from the results presented here and elsewhere[6,13] that protonation reactions of the 13-vertex metalla(carborane) salts **6** are characterized by initial retention of the docosahedral cage structure, now bearing a CH_2R substituent, but that this group is often readily lost along with the boron atom cage vertex to which it is attached. Facile 13-vertex to 12-vertex cage degradation reactions of this kind are extremely rare, particularly under acidic reaction conditions.[14] There is, however, a delicate balance between the 12- and 13-vertex cage structures which appears to be significantly, but not solely, affected by the nature of the groups attached to the metal vertex.

---

(13) Brew, S. A.; Carr, N.; Mortimer, M. D.; Stone, F. G. A. *J. Chem. Soc., Dalton Trans.* **1991**, 811.

(14) Maxwell, W. M.; Grimes, R. N. *Inorg. Chem.* **1979**, *18*, 2174.

Experimental Section

General Considerations. All reactions were carried out under an atmosphere of dry nitrogen, using Schlenk-line techniques. Solvents were distilled from appropriate drying agents under nitrogen before use. Petroleum ether refers to that fraction of bp 40–60 °C. Chromatography columns (ca. 15 cm in length and 2 cm in diameter) were packed with either alumina (Brockmann activity II) or silica gel (Aldrich, 70–230 mesh). The acid $HBF_4{\cdot}Et_2O$ was used as purchased from Aldrich Chemical Co. as an 85% solution in Et_2O. The compounds $[W(\equiv CMe)Br(CO)_2(NC_5H_4Me\text{-}4)_2]$,[15] $[NEt_4][W(\equiv CC_6H_4Me\text{-}4)(CO)_2(\eta^6\text{-}7,9\text{-}Me_2\text{-}7,9\text{-}C_2B_{10}H_{10})]$ (**6a**),[7] and $[N(PPh_3)_2][WI(CO)_3(\eta^5\text{-}7,9\text{-}Me_2\text{-}7,9\text{-}C_2B_9H_9)]$ (**7b**)[6] were prepared as previously described. The salts $[Y][W(\equiv CC_6H_4Me\text{-}4)(CO)_2(\eta^6\text{-}7,9\text{-}C_2B_{10}H_{12})]$ $\{Y = NEt_4$ or $N(PPh_3)_2\}$ (**6b**) were prepared from $[W(\equiv CC_6H_4Me\text{-}4)(CO)_2(O_2CCF_3)(NC_5H_4Me\text{-}4)_2]$ and $Na_2[7,9\text{-}C_2B_{10}H_{12}]$ by the method described for **6a**.

Instrumentation. NMR spectra were recorded at ambient temperatures, unless otherwise stated, using a Bruker AMX 360 spectrometer. The chemical shifts for ^1H and $^{13}C\{^1H\}$ spectra are referenced to $SiMe_4$; those for the ^{11}B and $^{31}P\{^1H\}$ spectra, measured in CD_2Cl_2, are positive to high frequency of $BF_3{\cdot}Et_2O$ (external) and 85% H_3PO_4 (external), respectively. Infrared spectra were measured with a Bruker IFS 25 FT-IR spectrometer.

Synthesis of the Salts $[NEt_4][W(\equiv CMe)(CO)_2(\eta^6\text{-}7,9\text{-}Me_2\text{-}7,9\text{-}C_2B_{10}H_{10})]$ (6c) and $[NEt_4][W(\equiv CMe)(CO)_2(\eta^6\text{-}7,9\text{-}C_2B_{10}H_{12})]$ (6d). A solution of $Na_2[7,9\text{-}Me_2\text{-}7,9\text{-}C_2B_{10}H_{10}]$ [generated in situ from $1,2\text{-}C_2B_{10}H_{10}Me_2$ (0.80 g, 4.65 mmol), Na metal (0.5 g, 21.75 mmol), and naphthalene (0.04 g, 0.31 mmol)] in THF (10 mL) was added to a solution of $[W(\equiv CMe)Br(CO)_2(NC_5H_4Me\text{-}4)_2]$ (2.00 g, 3.75 mmol) in THF (15 mL), and the resulting mixture was stirred for 2 h, after which $[NEt_4]Cl{\cdot}H_2O$ (0.79 g, 0.43 mmol) was added and stirring was continued for a further 1 h. Volatile materials were removed in vacuo, the residue extracted with CH_2Cl_2 (20 mL), and the extract filtered through a Celite plug. The volume of solvent was reduced in vacuo to ca. 8 mL and the solution chromatographed on a short (4 cm) column at ca. −20 °C. Elution with CH_2Cl_2 gave a bright yellow solution from which the solvent was removed in vacuo and the oily residue was washed with Et_2O (2 × 15 mL) at −78 °C to give $[NEt_4][W(\equiv CMe)(CO)_2(\eta^6\text{-}7,9\text{-}Me_2\text{-}7,9\text{-}C_2B_{10}H_{10})]$ (1.92 g) (**6c**) as a yellow powder. By a similar procedure $Na_2[7,9\text{-}C_2B_{10}H_{12}]$ (3.47 mmol), $[W(\equiv CMe)Br(CO)_2(NC_5H_4Me\text{-}4)_2]$ (3.02 mmol), and $[NEt_4]Cl{\cdot}H_2O$ (3.22 mmol) gave $[NEt_4][W(\equiv CMe(CO)_2(\eta^6\text{-}7,9\text{-}C_2B_{10}H_{12})]$ (1.11 g) (**6d**). Infrared and ^1H and $^{13}C\{^1H\}$ NMR data for these new alkylidyne species are given in Tables I and II.

Protonation Reactions Involving 1 Mol Equiv of Acid. (i) A CH_2Cl_2 (15 mL) solution containing $[NEt_4][W(\equiv CC_6H_4\text{-}Me\text{-}4)(CO)_2(\eta^6\text{-}7,9\text{-}Me_2\text{-}7,9\text{-}C_2B_{10}H_{10})]$ (**6a**) (0.19 g, 0.38 mmol) was saturated with CO at ca. −78 °C and treated with $HBF_4{\cdot}Et_2O$ (48 μL, 0.31 mmol). After the mixture was allowed to warm to ambient temperature the resulting yellow solution was evaporated to dryness in vacuo and the residue extracted with CH_2Cl_2–petroleum ether (1:1, 5 mL). The extract was transferred to the top of a silica gel chromatography column held at −20 °C. Elution with the same solvent mixture gave a yellow solution, from which the solvent was removed in vacuo and the residue taken up in *n*-hexane (5 mL). Cooling of this solution (ca. −30 °C) gave a yellow powder (0.14 g); NMR measurements on freshly prepared samples showed it to be composed mainly of $[W(CO)_4\{\eta^6\text{-}7,9\text{-}Me_2\text{-}7,9\text{-}C_2B_{10}H_9\text{-}11\text{-}(CH_2C_6H_4Me\text{-}4)\}]$ (**8a**) with a trace (ca. 5%) of $[W(CO)_4(\eta^5\text{-}7,9\text{-}Me_2\text{-}7,9\text{-}C_2B_9H_9)]$ (**9a**). Analytically pure samples of **8a** were obtained by cooling (ca. −30 °C) a saturated solution of the above mixture in *n*-hexane for 1 week.

(ii) Similarly, a CH_2Cl_2 (15 mL) solution containing **6a** (0.26 g, 0.41 mmol) and $PhC\equiv CPh$ (0.15 g, 0.84 mmol) was cooled to ca. −50 °C and treated with $HBF_4{\cdot}Et_2O$ (64 μL, 0.41 mmol). When the solution was warmed to room temperature the solvent was removed in vacuo, the residue extracted with CH_2Cl_2–petroleum ether (1:4, 5 mL), and the extract transferred to a silica gel chromatography column held at −20 °C. Eluting the column with the same solvent mixture removed a purple fraction along with an orange fraction. The two fractions could not be completely separated, and consequently spectroscopic measurements on the two fractions showed that each one contained a trace of the other. The orange solution thus obtained was shown to contain initially mainly $[W(CO)_2(\eta\text{-}PhC_2Ph)\{\eta^6\text{-}7,9\text{-}Me_2\text{-}7,9\text{-}C_2B_{10}H_9\text{-}11\text{-}(CH_2C_6H_4Me\text{-}4)\}]$ (**8b**) while the purple solution was composed primarily of $[W(CO)_2(\eta\text{-}PhC_2Ph)(\eta^5\text{-}7,9\text{-}Me_2\text{-}7,9\text{-}C_2B_9H_9)]$ (**9b**). The former complex slowly converts to the latter as described below.

(iii) By employing similar methodology, $[NEt_4][W(\equiv CMe)(CO)_2(\eta^6\text{-}7,9\text{-}Me_2\text{-}7,9\text{-}C_2B_{10}H_{10})]$ (**6c**) (0.19 g, 0.33 mmol), $PhC\equiv CPh$ (0.06 g, 0.34 mmol), and $HBF_4{\cdot}Et_2O$ (55 μL, 0.35 mmol) gave a purple eluate composed mainly of **9b** and a red solution containing mainly $[W(CO)_2(\eta\text{-}PhC_2Ph)\{\eta^6\text{-}7,9\text{-}Me_2\text{-}7,9\text{-}C_2B_{10}H_9\text{-}11\text{-}Et\}]$ (**8c**).

(iv) The salt $[NEt_4][W(\equiv CC_6H_4Me\text{-}4)(CO)_2(\eta^6\text{-}7,9\text{-}Me_2\text{-}7,9\text{-}C_2B_{10}H_{10})]$ (**6a**) (0.27 g, 0.42 mmol) was dissolved in CH_2Cl_2 (15 mL) and cooled to ca. −78 °C. The reagent $HBF_4{\cdot}Et_2O$ (66 μL, 0.42 mmol) was added and the mixture allowed to warm to ambient temperature, after which the material was preadsorbed onto silica gel for column chromatography at −20 °C. Elution of the column with CH_2Cl_2–petroleum ether (1:1) gave a yellow fraction which was reduced in volume in vacuo to ca. 5 mL, petroleum ether (15 mL) was added, and the resulting solution was cooled to ca. −30 °C for 3 d to give $[W(CO)_4(\eta^5\text{-}7,9\text{-}Me_2\text{-}7,9\text{-}C_2B_9H_9)]$ (**9a**) as a yellow powder (0.07 g). Employing $[NEt_4][W(\equiv CMe)(CO)_2(\eta^6\text{-}7,9\text{-}Me_2\text{-}7,9\text{-}C_2B_{10}H_{10})]$ (**6c**) in place of **6a** gives the same compound (36% yield), as evidenced by NMR measurements.

(v) To a cooled (ca. −78 °C) CH_2Cl_2 (20 mL) solution containing **6a** (0.15 g, 0.23 mmol) and PPh_3 (0.12 g, 0.46 mmol) was added $HBF_4{\cdot}Et_2O$ (36 μL, 0.23 mmol) and the resulting mixture allowed to warm to room temperature. After being preadsorbed onto silica gel (ca. 3 g) the residue was transferred to a silica gel chromatography column held at −20 °C. Eluting the column with CH_2Cl_2–petroleum ether (2:1) removed a bright yellow fraction which yielded yellow *microcrystals* of $[W(CO)_2(PPh_3)_2(\eta^5\text{-}7,9\text{-}Me_2\text{-}7,9\text{-}C_2B_9H_9)]$ (**9c**) (0.20 g), after reducing the volume of solvent in vacuo to ca. 2 mL and addition of petroleum ether (12 mL). The same species was obtained from **6c** (0.12 g, 0.21 mmol), PPh_3 (0.11 g, 0.42 mmol), and $HBF_4{\cdot}Et_2O$ (33 μL, 0.21 mmol) by employing a similar method.

(vi) The salt $[NEt_4][W(\equiv CMe)(CO)_2(\eta^6\text{-}7,9\text{-}C_2B_{10}H_{12})]$ (**6d**) (0.16 g, 0.30 mmol) and PPh_3 (0.16 g, 0.63 mmol) were dissolved in CH_2Cl_2 (20 mL), and the solution was cooled to ca. −78 °C. The acid $HBF_4{\cdot}Et_2O$ (48 μL, 0.31 mmol) was added and the solution allowed to warm to room temperature. Stirring was continued for a further 2 h, after which the solution was preadsorbed onto silica gel and transferred to a silica gel chromatography column held at −20 °C. Elution with CH_2Cl_2–petroleum ether (2:1) gave a lime green solution which was reduced in volume in vacuo to ca. 5 mL, and petroleum ether (20 mL) was added. The volume was again reduced in vacuo until a yellow powder precipitated. This was collected, washed with petroleum ether (2 × 10 mL), and dried in vacuo to give $[W(CO)_2(PPh_3)_2(\eta^5\text{-}7,9\text{-}C_2B_9H_{11})]$ (**9d**) (0.13 g).

Thermal Transformation Reactions of the 13-Vertex Carborane Complexes. (i) Essentially pure $[W(CO)_4\{\eta^6\text{-}7,9\text{-}Me_2\text{-}7,9\text{-}C_2B_{10}H_9\text{-}11\text{-}(CH_2C_6H_4Me\text{-}4)\}]$ (**8a**) (0.20 g), obtained as described above, was dissolved in CH_2Cl_2 (15 mL) and the mixture allowed to stand at ca. 25 °C for 2 weeks, after which time IR measurements showed no bands due to the starting complex. Volatile material was removed in vacuo and the residue extracted with *n*-hexane (15 mL) and cooled to ca. −30 °C to give yellow *microcrystals* of $[W(CO)_4(\eta^5\text{-}7,9\text{-}Me_2\text{-}7,9\text{-}C_2B_9H_9)]$ (**9a**) (0.12 g, ca. 75% yield).

(ii) A solution containing predominantly $[W(CO)_2(\eta\text{-}PhC_2Ph)\{\eta^6\text{-}7,9\text{-}Me_2\text{-}7,9\text{-}C_2B_{10}H_9\text{-}11\text{-}(CH_2C_6H_4Me\text{-}4)\}]$ (**8b**) (0.18 g) in CH_2-

---

[15] Brew, S. A.; Jenkins, P. D.; Jeffery, J. C.; Stone, F. G. A. *J. Chem. Soc., Dalton Trans.* **1992**, 401.

Cl_2 (20 mL), obtained as described above, was heated at reflux temperature for 24 h. Volatile material was removed in vacuo, the residue was extracted with CH_2Cl_2–petroleum ether (1:4, 6 mL), and the extracts were chromatographed on silica gel at −20 °C. Elution with the same solvent mixture gave a deep purple solution from which purple *microcrystals* of $[W(CO)_2(\eta\text{-}PhC_2Ph)(\eta^5\text{-}7,9\text{-}Me_2\text{-}7,9\text{-}C_2B_9H_9)]$ (**9b**) (0.12 g, ca. 80% yield) were obtained by cooling the solution to ca. −30 °C. A similar experiment employing $[W(CO)_2(\eta\text{-}PhC_2Ph)\{\eta^6\text{-}7,9\text{-}Me_2\text{-}7,9\text{-}C_2B_{10}H_9\text{-}11\text{-}Et\}]$ (**8c**) led to decomposition to uncharacterized species with only a trace amount of **9b** being obtained.

Reaction between $[N(PPh_3)_2][WI(CO)_3(\eta^5\text{-}7,9\text{-}Me_2\text{-}7,9\text{-}C_2B_9H_9)]$ (7b) and PPh_3. The compound $[N(PPh_3)_2][WI(CO)_3(\eta^5\text{-}7,9\text{-}Me_2\text{-}7,9\text{-}C_2B_9H_9)]$ (**7b**) (0.11 g, 0.10 mmol), PPh_3 (0.06 g, 0.23 mmol), and $TlBF_4$ (0.04 g, 0.14 mmol) were dissolved/suspended in CH_2Cl_2 (15 mL), and the resulting mixture was stirred for 5 d. The solution was then filtered through a Celite pad, preadsorbed onto silica gel, and transferred to the top of a silica gel chromatography column held at −20 °C. Eluting the column with CH_2Cl_2–petroleum ether (1:1) gave a yellow solution which upon reduction of volume in vacuo to ca. 5 mL gave yellow *crystals* of $[W(CO)_2(PPh_3)_2(\eta^5\text{-}7,9\text{-}Me_2\text{-}7,9\text{-}C_2B_9H_9)]$ (**9c**) (0.04 g, 43% yield).

Protonation Reactions Involving 0.5 Mol Equiv of Acid. (i) A rapidly stirred CH_2Cl_2 (15 mL) solution of $[NEt_4][W(\equiv CC_6H_4Me\text{-}4)(CO)_2(\eta^6\text{-}7,9\text{-}Me_2\text{-}7,9\text{-}C_2B_{10}H_{10})]$ (**6a**) (0.21 g, 0.33 mmol) was cooled to ca. −78 °C and treated with $HBF_4{\cdot}Et_2O$ (17 μL, 0.11 mmol). The resulting dark colored solution was slowly (ca. 1 h) allowed to warm to ambient temperature before being evaporated to dryness under vacuo. The residue was extracted with CH_2Cl_2–petroleum ether (2:1, 5 mL), and the extracts were transferred to the top of a silica gel chromatography column. Eluting the column with the same solvent mixture gave a deep purple fraction followed by a slower moving green eluate. The purple solution was reduced in volume in vacuo to ca. 5 mL, and petroleum ether (15 mL) was added to give an intense purple powder (0.02 g). The green solution was evaporated to dryness in vacuo, and the oily residue was dissolved in CH_2Cl_2 (5 mL). Slow diffusion of Et_2O (15 mL) into this solution gave $[NEt_4][W_2\{\mu\text{-}\eta^2\text{-}C(C_6H_4Me\text{-}4)CO\}(CO)_3(\eta^6\text{-}7,9\text{-}Me_2\text{-}7,9\text{-}C_2B_{10}H_{10})\{\eta^6\text{-}7,9\text{-}Me_2\text{-}7,9\text{-}C_2B_{10}H_9\text{-}11\text{-}(CH_2C_6H_4Me\text{-}4)\}]$ (**10a**) as a green powder (0.04 g).

(ii) A solution containing $[NEt_4][W(\equiv CC_6H_4Me\text{-}4)(CO)_2(\eta^6\text{-}7,9\text{-}C_2B_{10}H_{12})]$ (**6b**) (0.29 g, 0.47 mmol) in CH_2Cl_2 (15 mL) was cooled to ca. −78 °C, and $HBF_4{\cdot}Et_2O$ (30 μL, 0.19 mmol) was rapidly added. The resulting solution was allowed to warm to ambient temperature over a period of 1 h and then preadsorbed onto silica gel (ca. 3 g) and transferred to the top of a silica gel chromatography column held at ca. −20 °C. Elution of the column with CH_2Cl_2–petroleum ether (3:1) gradually increasing in polarity to pure CH_2Cl_2 gave a green solution which was reduced in volume in vacuo to ca. 5 mL and petroleum ether added to give green *microcrystals* of $[NEt_4][W_2\{\mu\text{-}\eta^2\text{-}C(C_6H_4Me\text{-}4)CO\}(CO)_3(\eta^6\text{-}7,9\text{-}C_2B_{10}H_{12})\{\eta^6\text{-}7,9\text{-}C_2B_{10}H_{11}\text{-}11\text{-}(CH_2C_6H_4Me\text{-}4)\}]$ (**10b**) (0.06 g).

(iii) Treatment of a solution of $[NEt_4][W(\equiv CMe)(CO)_2(\eta^6\text{-}7,9\text{-}Me_2\text{-}7,9\text{-}C_2B_{10}H_{10})]$ (**6c**) (0.31 g, 0.54 mmol) in CH_2Cl_2 (15 mL) held at ca. −78 °C with $HBF_4{\cdot}Et_2O$ (34 μL, 0.22 mmol) gave a dark colored solution which was allowed to warm to ambient temperature over a period of ca. 1 h before being preadsorbed onto silica gel and transferred to the top of a silica gel chromatography column held at −20 °C. Eluting the column with CH_2Cl_2–petroleum ether (4:1) first removed a deep purple fraction, the volume of which was reduced to ca. 5 mL, and petroleum ether (15 mL) added to give a purple powder (0.03 g). Continued treatment of the column with the same solvent mixture then removed a green solution which was reduced in volume to ca. 5 mL and treated with petroleum ether (20 mL) to give green *microcrystals* of $[NEt_4][W_2\{\mu\text{-}\eta^2\text{-}C(Me)CO\}(CO)_3(\eta^6\text{-}7,9\text{-}Me_2\text{-}7,9\text{-}C_2B_{10}H_{10})\{\eta^6\text{-}7,9\text{-}Me_2\text{-}7,9\text{-}C_2B_{10}H_9\text{-}11\text{-}Et\}]$ (**10c**) (0.06 g).

(iv) Similarly, $[NEt_4][W(\equiv CMe)(CO)_2(\eta^6\text{-}7,9\text{-}C_2B_{10}H_{12})[$ (**6d**) (0.13 g, 0.24 mmol) and $HBF_4{\cdot}Et_2O$ (19 μL, 0.12 mmol) gave after column chromatography eluting with CH_2Cl_2–petroleum ether (3:1) green *microcrystals* of $[NEt_4][W_2\{\mu\text{-}\eta^2\text{-}C(Me)CO\}(CO)_3(\eta^6\text{-}7,9\text{-}C_2B_{10}H_{12})\{\eta^6\text{-}7,9\text{-}C_2B_{10}H_{11}\text{-}11\text{-}Et\}]$ (**10d**) (0.02 g).

Table V. Crystallographic Data for 10c [Y = Au(PPh$_3$)$_2$][a]

cryst dimens/mm	1.40 × 0.53 × 0.34
formula	$C_{54}H_{69}AuB_{20}O_4P_2W_2{\cdot}CH_2Cl_2$
M_r	1709.8
cryst color, shape	green prism
cryst system	triclinic
space group (no.)	$P\bar{1}$ (No. 2)
a/Å	9.398(1)
b/Å	18.181(5)
c/Å	20.491(3)
α/deg	69.07(2)
β/deg	88.75(1)
γ/deg	85.91(1)
V/Å^3	3256.7(11)
Z	2
d_{calcd}/g cm^{-3}	1.744
μ(Mo K$_\alpha$)/cm^{-1}	60.2
F(000)/e	1648
2θ range/deg	3–40
T/K	292
no. of reflns meas	6806
no. of unique reflns	6034
no. of observed reflns	5562
criterion for observed $n[F_o \geq n\sigma(F_o)]$	$n = 4$
R (R')[b]	0.0463 (0.0603)
final electron density diff features (max/min)/e Å^{-3}	2.36/−2.13
S (goodness-of-fit)	1.2

[a] Data collected on an Enraf Nonius CAD4-F automated diffractometer operating in the $\omega - 2\theta$ scan mode (h, 0–9; k, −17 to 17; l, −19 to 19); graphite-monochromated Mo K$_\alpha$ X-radiation, $\bar{\lambda}$ = 0.710 73 Å. Refinement was by block full-matrix least-squares on F with a weighting scheme of the form $w^{-1} = [\sigma^2(F_o) + 0.00054|F_o|^2]$ where $\sigma_c^2(F_o)$ is the variance in F_o due to counting statistics. [b] $R = \sum||F_o| - |F_c||/\sum|F_o|$, $R' = \sum w^{1/2}||F_o| - |F_c||/\sum w^{1/2}|F_o|$.

Reaction between $[NEt_4][W_2\{\mu\text{-}\eta^2\text{-}C(Me)CO\}(CO)_3(\eta^6\text{-}7,9\text{-}Me_2\text{-}7,9\text{-}C_2B_{10}H_{10})\{\eta^6\text{-}7,9\text{-}Me_2\text{-}7,9\text{-}C_2B_{10}H_9\text{-}11\text{-}Et\}]$ (10c) and $[AuCl(PPh_3)]$. The compounds **10c** (0.12 g, 0.13 mmol), $[AuCl(PPh_3)]$ (0.06 g, 0.12 mmol), and $TlBF_4$ (0.04 g, 0.14 mmol) were dissolved/suspended in THF (15 mL), and the resulting mixture was rapidly stirred for 4 d. After volatile materials were removed in vacuo, the residue was extracted with CH_2Cl_2 (5 mL), and the extracts were chromatographed on alumina. Eluting with CH_2Cl_2 separated two green fractions, the latter of which was shown by IR and NMR measurements to be unchanged starting material. The other green solution was reduced in volume in vacuo to 2 mL, and petroleum ether was allowed to diffuse into the solution at ca. −20 °C to give green *crystals* of $[Au(PPh_3)_2][W_2\{\mu\text{-}\eta^2\text{-}C(Me)CO\}(CO)_3(\eta^6\text{-}7,9\text{-}Me_2\text{-}7,9\text{-}C_2B_{10}H_{10})\{\eta^6\text{-}7,9\text{-}Me_2\text{-}7,9\text{-}C_2B_{10}H_9\text{-}11\text{-}Et\}]$ (0.04 g, 20% yield) [$\delta(^{31}P)$ 45.5 ppm]. Proton and $^{13}C\{^1H\}$ NMR measurements revealed that the anion of this complex has the same structure as that in the starting complex **10c**.

Crystal Structure Determination. Crystals of the compound $[Au(PPh_3)_2][W_2\{\mu\text{-}\eta^2\text{-}C(Me)CO\}(CO)_3(\eta^6\text{-}7,9\text{-}Me_2\text{-}7,9\text{-}C_2B_{10}H_{10})\{\eta^6\text{-}7,9\text{-}Me_2\text{-}7,9\text{-}C_2B_{10}H_9\text{-}11\text{-}Et\}]$ suitable for analysis by X-ray diffraction were grown by the slow (1 week) diffusion of petroleum ether into a CH_2Cl_2 solution of the complex at ca. −20 °C. The crystal data and other experimental details are listed in Table V. Final cell dimensions used in the data collection and refinement of the structure were determined from the setting angle values of 25 accurately centered reflections. Three standard reflections measured every 2 h showed no significant variation over the period of the data collection (<0.4%). After deletion of these check intensity data as well as the systematic absences, averaging of duplicate and equivalent measurements was performed and the data were corrected for Lorentz, polarization and X-ray absorption effects. The absorption correction was based on an empirical method employing 10 high angle ψ data.

The metal atom positions were determined by the Patterson method, all other non-hydrogen atoms being located from successive difference Fourier syntheses. Non-hydrogen atoms were allowed to refine freely with anisotropic thermal parameters.

Table VI. Atomic Coordinates (× 10^4) and Equivalent Isotropic Displacement Parameters (Å^3 × 10^3) for 10c [Y = Au(PPh_3)$_2$]

name	x	y	z	U(eq)[a]	name	x	y	z	U(eq)[a]
W(1)	2962(1)	3158(1)	1048(1)	36(1)	Au	5451(1)	2350(1)	6744(1)	45(1)
C(11)	1651(14)	3598(8)	206(8)	60(3)	P(1)	5194(3)	2659(2)	5552(2)	45(1)
O(11)	953(10)	3820(7)	–283(5)	86(3)	C(41)	4024(13)	3505(8)	5236(6)	63(3)
C(12)	4435(12)	3384(7)	269(7)	51(3)	C(42)	3994(20)	4087(10)	5559(10)	115(3)
O(12)	5254(11)	3499(6)	–163(5)	90(3)	C(43)	3106(17)	4791(9)	5290(10)	100(3)
C(1)	4752(11)	3288(6)	1648(6)	47(3)	C(44)	2161(16)	4927(9)	4768(8)	87(3)
B(2)	4245(14)	4193(9)	1231(8)	58(3)	C(45)	2270(18)	4391(9)	4414(11)	132(3)
C(3)	2510(12)	4502(6)	1108(7)	53(3)	C(46)	3028(13)	3683(9)	4700(8)	92(3)
B(4)	1270(14)	3876(9)	1502(7)	52(3)	C(51)	4446(12)	1909(6)	5330(5)	41(3)
B(5)	2015(12)	2981(8)	2111(6)	44(3)	C(52)	3176(13)	1592(9)	5674(7)	72(3)
B(6)	3965(15)	2764(9)	2225(7)	57(3)	C(53)	2503(15)	1000(9)	5505(8)	88(3)
B(7)	3492(15)	4732(8)	1700(8)	61(3)	C(54)	3124(15)	747(10)	4995(8)	94(3)
B(8)	1630(13)	4642(8)	1780(7)	49(3)	C(55)	4315(14)	1083(8)	4650(8)	76(3)
B(9)	1317(15)	3713(8)	2386(8)	59(3)	C(56)	5004(12)	1596(7)	4852(6)	56(3)
B(10)	2967(14)	3226(8)	2760(7)	47(3)	C(61)	6819(12)	2867(6)	5043(5)	46(3)
B(11)	4334(16)	3809(8)	2250(8)	63(3)	C(62)	6803(12)	3323(9)	4349(5)	81(3)
B(12)	2765(16)	4180(9)	2537(10)	76(3)	C(63)	8020(12)	3421(8)	3972(7)	78(3)
C(2)	6378(11)	3105(7)	1542(8)	73(3)	C(64)	9282(13)	3086(10)	4299(8)	96(3)
C(4)	2256(12)	5163(7)	413(6)	64(3)	C(65)	9346(15)	2650(12)	4988(10)	153(3)
W(2)	1895(1)	1743(1)	1888(1)	33(1)	C(66)	8141(16)	2549(13)	5397(10)	161(3)
C(13)	393(12)	2341(7)	1200(6)	45(3)	P(2)	5222(3)	2266(2)	7889(2)	41(1)
O(13)	–557(8)	2588(5)	836(4)	60(2)	C(71)	6798(9)	2228(5)	8375(5)	33(3)
C(5)	1032(10)	764(6)	1636(6)	43(3)	C(72)	7886(10)	1669(6)	8403(6)	59(3)
B(22)	2521(15)	380(7)	2002(7)	51(3)	C(73)	9141(12)	1647(9)	8746(9)	89(3)
C(6)	3042(10)	498(6)	2724(5)	41(3)	C(74)	9328(12)	2134(7)	9118(6)	52(3)
B(24)	1968(12)	1024(7)	3110(6)	39(3)	C(75)	8264(13)	2702(8)	9105(7)	80(3)
B(25)	89(12)	1229(7)	2837(6)	40(3)	C(76)	7016(15)	2756(8)	8703(7)	80(3)
B(26)	–272(13)	973(8)	2085(7)	49(3)	C(81)	4279(10)	1405(6)	8425(5)	41(3)
B(27)	2329(14)	–32(9)	3511(7)	57(3)	C(82)	4298(14)	1182(8)	9165(8)	72(3)
B(28)	628(14)	377(8)	3545(7)	52(3)	C(83)	3544(15)	539(10)	9527(7)	81(3)
B(29)	–473(12)	291(7)	2936(7)	41(3)	C(84)	2829(13)	123(8)	9229(8)	70(3)
B(30)	645(15)	–88(8)	2347(7)	53(3)	C(85)	2816(14)	360(9)	8510(9)	81(3)
B(31)	2420(16)	–373(8)	2809(8)	64(3)	C(86)	3564(10)	1008(6)	8091(6)	45(3)
B(32)	882(15)	–467(9)	3288(9)	67(3)	C(91)	4151(12)	3132(7)	7859(6)	52(3)
C(7)	658(11)	730(7)	961(6)	54(3)	C(92)	4578(16)	3899(8)	7411(7)	74(3)
C(8)	4710(12)	459(7)	2793(7)	61(3)	C(93)	3719(15)	4562(8)	7385(7)	71(3)
C(9)	–903(11)	1895(7)	3013(7)	58(3)	C(94)	2466(16)	4520(8)	7752(8)	77(3)
C(10)	–2274(13)	1655(9)	3380(8)	85(3)	C(95)	2091(14)	3797(8)	8196(7)	88(3)
C(20)	3624(11)	1916(5)	1101(6)	41(3)	C(96)	2866(14)	3114(8)	8253(7)	74(3)
C(21)	5143(11)	1555(7)	1111(7)	59(3)	C(99)	–242(13)	7027(7)	2612(6)	150(3)
C(22)	2896(10)	2182(7)	490(6)	44(3)	Cl(1)	1077(12)	6268(6)	3052(6)	87(3)
O(22)	2466(10)	2192(5)	–34(4)	67(3)	Cl(2)	–930(14)	7554(7)	3145(6)	77(3)

[a] Equivalent isotropic U defined as one third of the trace of the orthogonalized U_{ij} tensor.

The atom H(5) was located in difference Fourier maps and allowed to ride on the parent boron atom B(5) with a fixed isotropic thermal parameter (U_{iso} 60 × 10^{-3}). All other hydrogen atoms were included at geometrically calculated positions (C–H 0.96 Å and B–H 1.10 Å) and allowed to ride on the parent carbon or boron atom with fixed isotropic thermal parameters (U_{iso} 80 × 10^{-3} and 60 × 10^{-3}, respectively). Calculations were performed using the SHELXTL-PC package of programs.[16] Atomic scattering factors are from ref 17. Final atomic positional parameters for the non-hydrogen atoms are given in Table VI.

Acknowledgment. We thank the Robert A. Welch Foundation for support (Grants AA-1201 and 0668) and Dr. S. A. Brew for helpful discussions.

Supplementary Material Available: Complete tables of bond lengths and angles, anisotropic thermal parameters, and hydrogen atom parameters (17 pages). Ordering information is given on any current masthead page.

OM920714L

---

(16) Siemens (1989). SHELXTL-PC Siemens X-ray Instruments, Madison, WI.

(17) *International Tables for X-ray Crystallography*; Kynoch Press; Birmingham, UK, 1974; Vol. 4.